Supplementary Material (ESI) for Organic & Biomolecular Chemistry

Supplementary Information

for

Molecular Assembly of A Squaraine Dye with Cationic Surfactant and Nucleotides: Its Impact on Aggregation and Fluorescence Response

Yongqian Xu, Andrey Malkovskiy, Qiuming Wang and Yi Pang*

Department of Chemistry & Maurice Morton Institute of Polymer Science, Department of Polymer Science, Department of Chemical and Biomolecular Engineering, The University of Akron, Akron, OH, 44325
yp5@uakron.edu

1. Materials and general procedure

All the solvents and reagents were of analytic grade and used as received. Water used was ultra filter deionized and purchased from Fisher Scientific. NMR spectra were collected on a Varian 300 Gemini spectrometer. Mass spectrometric data were obtained on a HP1100LC/MSD mass spectrometry. UV-Vis spectra were acquired on a Hewlett-Packard 8453 diode-array spectrometer. Fluorescence spectra were obtained on a HORIBA Jobin Yvon NanoLog spectrometer. HRMS data were performed on a TOF MS system. Dynamic light scattering (DLS) data was obtained on a Malvern Zetasizer Nano S (U.K., ZEN 3600) at 25 ^{o}C. AFM images were recorded under ambient conditions using a Park Scientific Autoprobe CP, which is operating in the tapping mode with Micromasch tapping probes with radius of curvature being <4 nm. The tips were brand new.

2. Synthesis of SQ

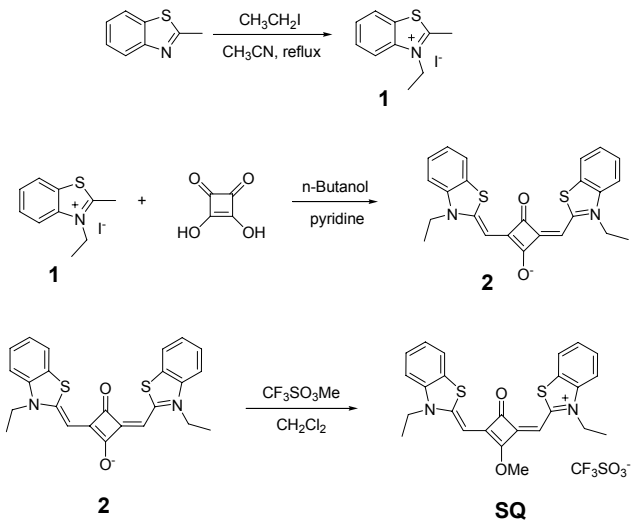

Synthesis of 3-Ethyl-2-methyl-1,3-benzothiazol-3-ium Iodide (**1**). A solution of 2-methylbenzothiazole (4.48 g, 30 mmol) and iodoethane 14.03 g, 90 mmol) in acetonitrile (250 mL) was heated under reflux for 24 h. After

cooling, diethyl ether (200 mL) was added, and the desired salt was collected by filtration under reduced pressure and washed several times with diethyl ether. The salt was dried under vacuum. The unreacted 2-methylbenzothiazole in filtrate was recovered by removal of ether, and further treated with additional iodoethane under reflux. The process was repeated 1~3 times to achieve a suitable yield of **1** as white solid (6.35 g, 69.4%). ^{1}H NMR (CD_3OD, 300 MHz) δ (ppm) 8.33 (d, 1H, J = 7.8 Hz), 8.30 (d, 1H, J = 8.4 Hz), 7.92 (dd, 1H, J = 7.8 Hz, J = 8.4 Hz), 7.81 (dd, 1H, J = 7.8 Hz, J = 8.4 Hz), 4.85 (q, 2H, J = 7.5 Hz), 3.27 (s, 3H), 1.60 (t, 3H, J = 7.5 Hz).

Synthesis of **2**. The solution of the quaternary ammonium salt (**1**) (0.92 g, 3 mmol) and squaric acid (0.17 g, 1.5 mmol) in BuOH/pyridine (v/v, 5/1) (60 mL) was heated at reflux for overnight. The product was purified on a silica gel column (by using CH_2Cl_2/MeOH as eluent) to give green solid (0.46 g, 70.7%). ^{1}H NMR ($CDCl_3$, 300 MHz) δ (ppm) 7.53 (d, 2H, J = 7.8 Hz), 7.35 (dd, 2H, J = 7.8 Hz, J = 8.4 Hz), 7.18 (dd, 2H, J = 7.8 Hz, J = 8.4 Hz), 7.12 (d, 2H, J = 8.4 Hz), 5.88 (s, 2H), 4.15 (q, 2H, 7.2 Hz), 1.43 (q, 6H, J = 7.2 Hz).

Synthesis of **SQ**. To a solution of **2** (172 mg, 0.4 mmol) in anhydrous CH_2Cl_2 (50 mL) was added $CF_3SO_3CH_3$ (261 mg, 1.6 mmol) at room temperature while the mixture was vigorously stirred under N_2 atmosphere. After stirring for 3~5 h, the mixture was quenched with cold 5% aqueous $NaHCO_3$ solution. The organic layer was dried with anhydrous Na_2SO_4 and the resulting residue was purified on a silica gel column (by using CH_2Cl_2/MeOH as eluent) to give **SQ** (195 mg, 82.3 %). ^{1}H NMR (DMSO-d_6, 300 MHz) δ (ppm) 8.04 (d, 2H, J = 7.8 Hz), 7.77 (d, 2H, J = 8.4 Hz), 7.58 (dd, 2H, J = 7.5 Hz , J = 8.4 Hz), 7.42 (dd, 2H, J = 7.2 Hz , J = 8.4 Hz), 6.06 (s, 2H), 4.54 (s, 3H), 4.47(q, 4H, J = 6.9 Hz), 1.29 (t, 6H, J = 6.9 Hz). ^{13}C NMR (DMSO-d_6, 75 MHz) δ (ppm) 161.96, 158.08, 140.57, 128.53, 127.98, 125.78, 123.51, 114.10, 85.57, 83.70, 61.28, 42.05, 13.10. HRMS (ESI+) found 448.1300 $(M)^+$, calcd for $C_{25}H_{23}N_2O_2S_2$ 448.1279

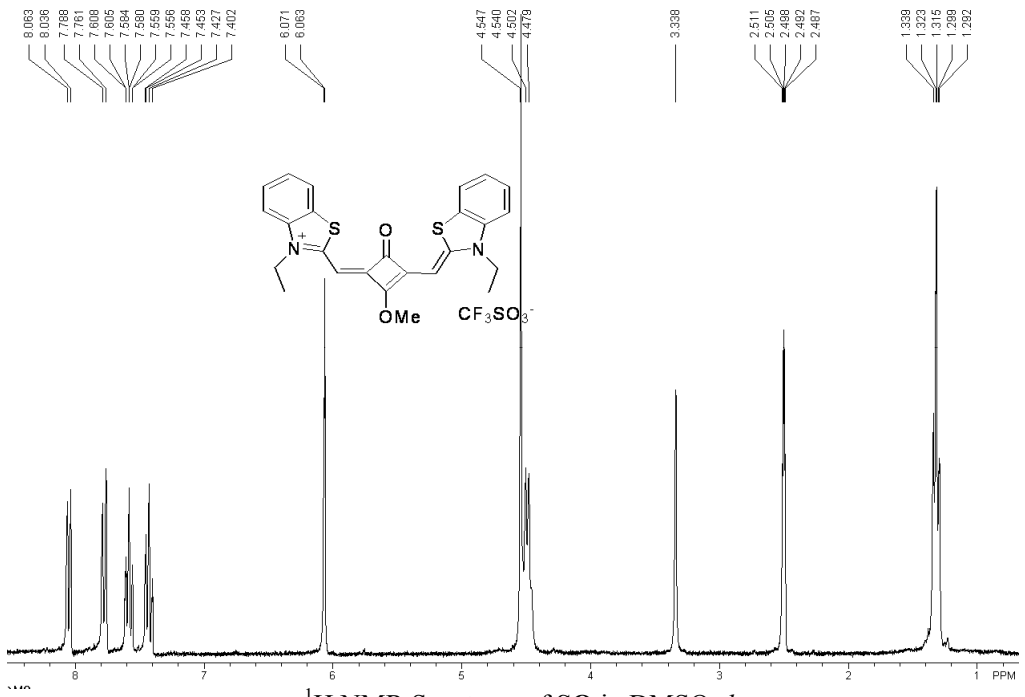

^{1}H NMR Spectrum of **SQ** in DMSO-d_6.

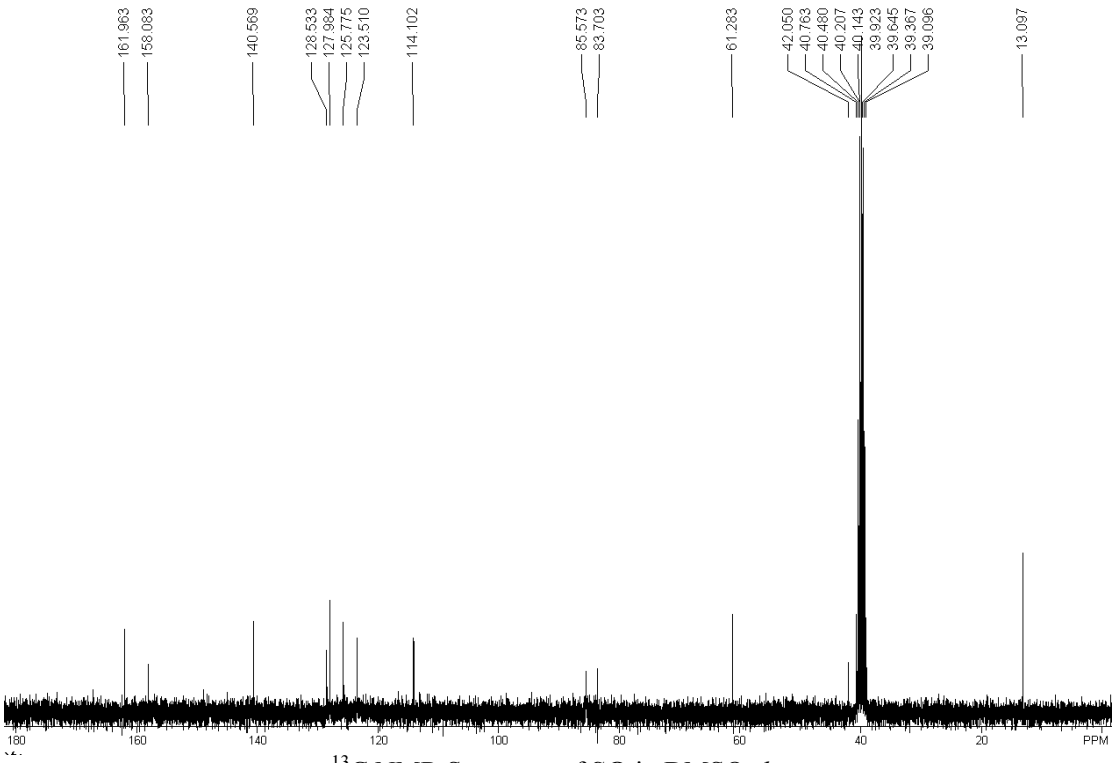

^{13}C NMR Spectrum of **SQ** in DMSO-d_6.

3. UV and fluorescence experiments

Stock solution (5.0×10^{-4} M) of **SQ** in ethanol, stock solution (1.0×10^{-2} M) of CTAB and all kind of anion ions in water were prepared. An aliquot (30 μL) of the **SQ** stock solution was added to 3 mL of 10 mM phosphate buffer solution (pH 7.20) in a quartz cuvette. The sample was gently stirred for 15 s before the UV and fluorescence was recorded. For the CTAB and anion ions, they were added in 10 μL increments to SQ solution.

4. Hill plot analysis for ATP-CTAB/SQ assembly interaction

Hill equation here is $\log[Y/(1-Y)] = n \log[ATP] + \log K_{app}$, where Y, n, [ATP] and K_{app} represent the fraction of ligand binding sites filled, Hill coefficient, ATP concentration and the apparent association constant, respectively. When appropriate, the value of Hill coefficient describes the cooperativity of ligand binding in the following way: $n > 1$, positive cooperativity; $n = 1$, noncooperativity; and $n < 1$, negative cooperativity.[S1] Y was determined by the equation of $(I-I_0)/(I_{max}-I_0)$, where I_0, I, and I_{max} are the fluorescence intensity at 676 nm in the absence and in the presence of excess amount of ATP.

S1. (a) S. Shinkai, M. Ikeda, A. Sugasaki and M. Takeuchi, *Acc. Chem. Res.*, 2001, **34**, 494. (b) G. Ercolani *J. Am. Chem. Soc.*, **2003**, *125*, 16097–16103.

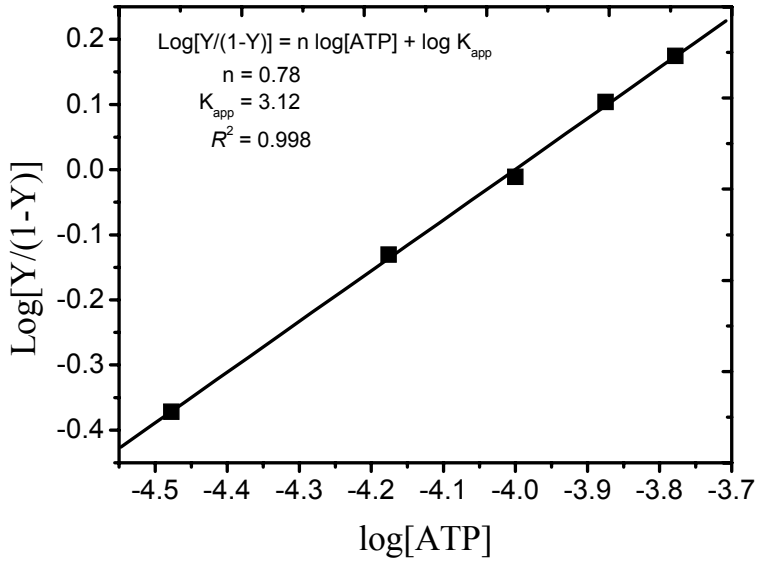

Fig. S1. Hill plot for interaction of ATP with CTAB-SQ ensemble in phosphate buffer solution (10 mM, pH 7.2) based on fluorescence intensity changes in low ATP concentration range.

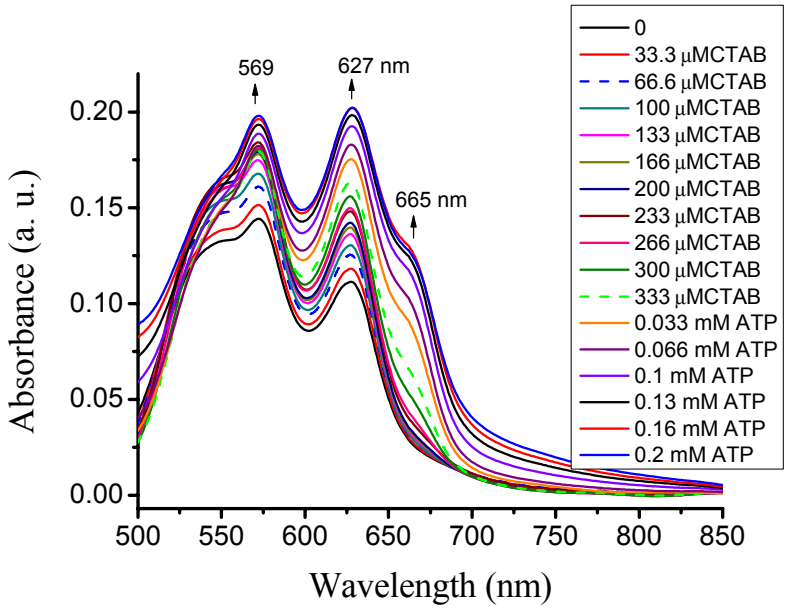

Figure S2. Absorption change of **SQ** (5 μM) in phosphate buffer (10 mM, pH 7.2) upon addition of CTAB, followed by ATP.

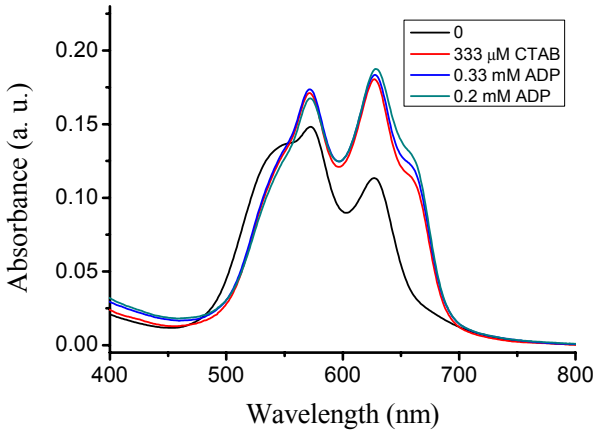

Figure S3. Absorption change of **SQ** (5 μM) in phosphate buffer (10 mM, pH 7.2) upon addition of CTAB, followed by ADP.

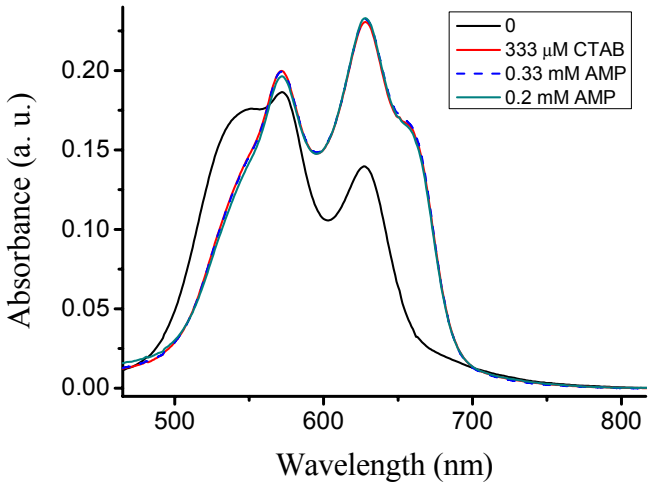

Figure S4. Absorption change of **SQ** (5 μM) in phosphate buffer (10 mM, pH 7.2) upon addition of CTAB, followed by AMP. The addition of AMP induced no spectral change.

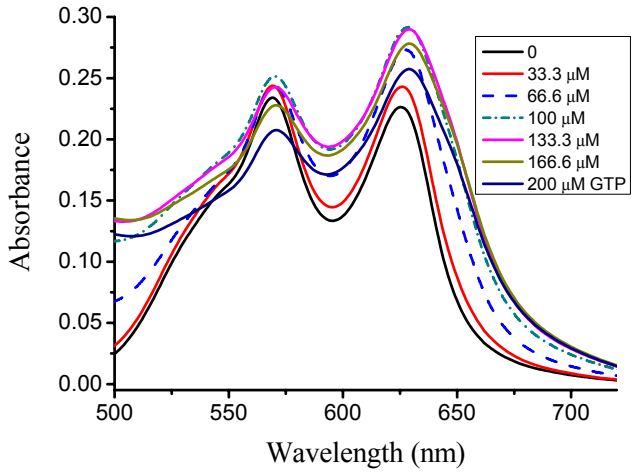

Figure S5. Absorption change of **SQ** (5 μM) in phosphate buffer (10 mM, pH 7.2) upon addition of GTP in the presence of 333 μM of CTAB.

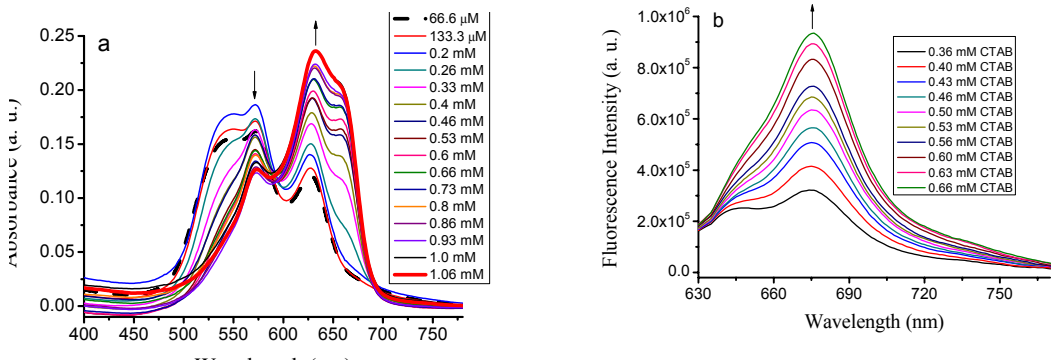

Figure S6. Absorption (a) and Fluorescence (b) change of **SQ** (5 μM) in phosphate buffer (10 mM, pH 7.2) upon addition of CTAB.

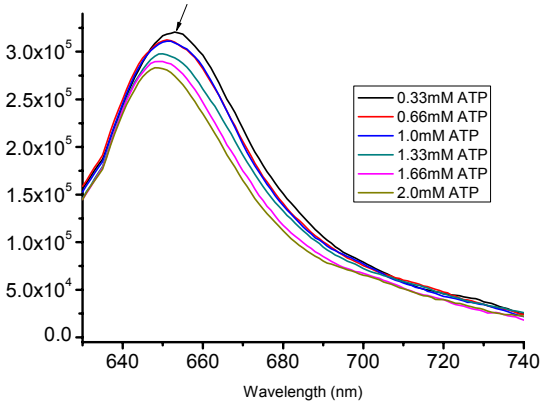

Figure S7. Fluorescence spectra of **SQ** (5 μM) in phosphate buffer (10 mM, pH 7.2) upon addition of ATP. The result shows that the system gives nearly no response in the absense of CTAB.

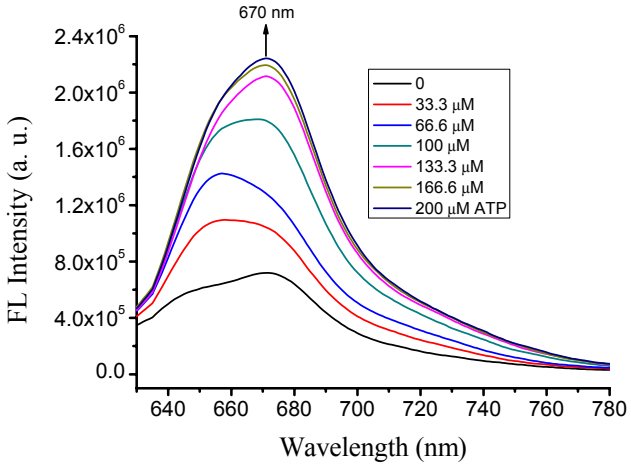

Figure S8. Fluorescence response of **SQ** (5 μM) in phosphate buffer (10 mM, pH 7.2) in the presence of CTAB (0.33 mM) upon addition of different amount of ATP.

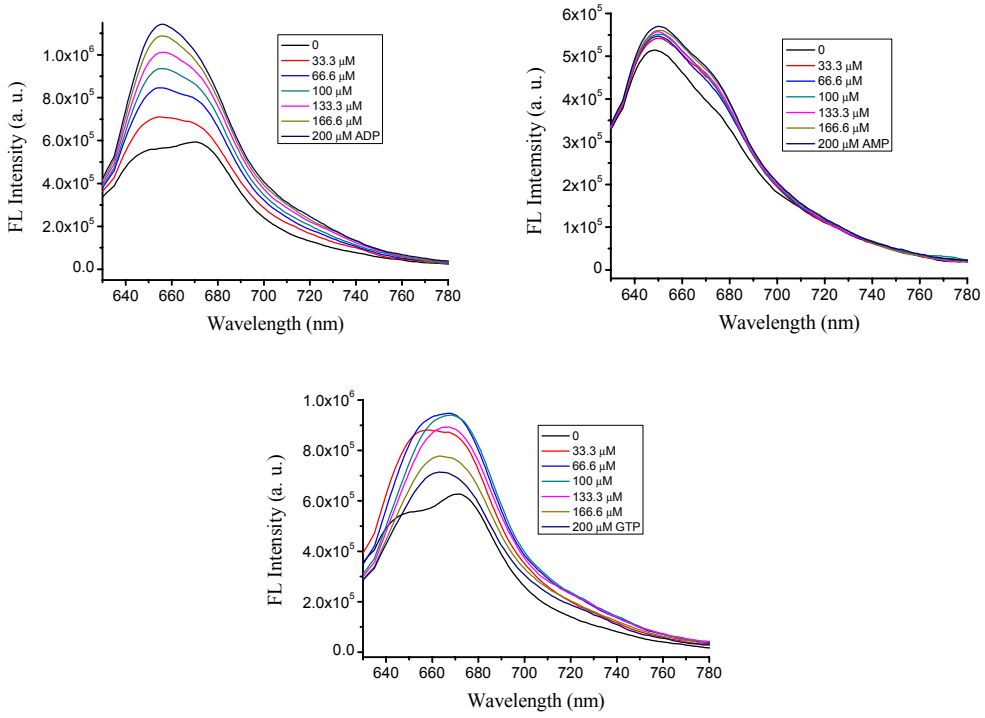

Figure S9. Fluorescence response of **SQ** (5 μM) in phosphate buffer (10 mM, pH 7.2) in the presence of CTAB (0.33 mM) upon addition of different anions.

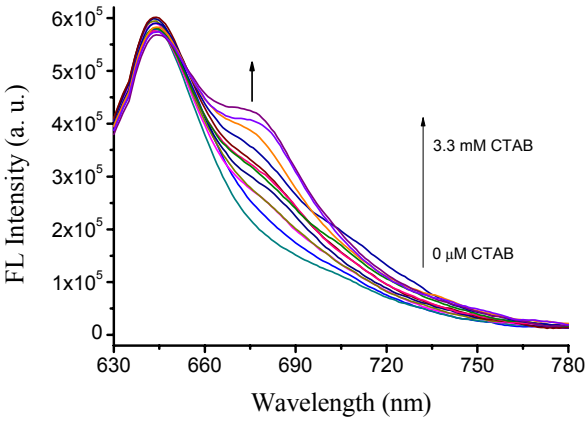

Figure S10. Fluorescence change of **SQ** (5 μM) in phosphate buffer (10 mM, pH 7.2) in the presence of ATP (300 μM) upon addition of CTAB.

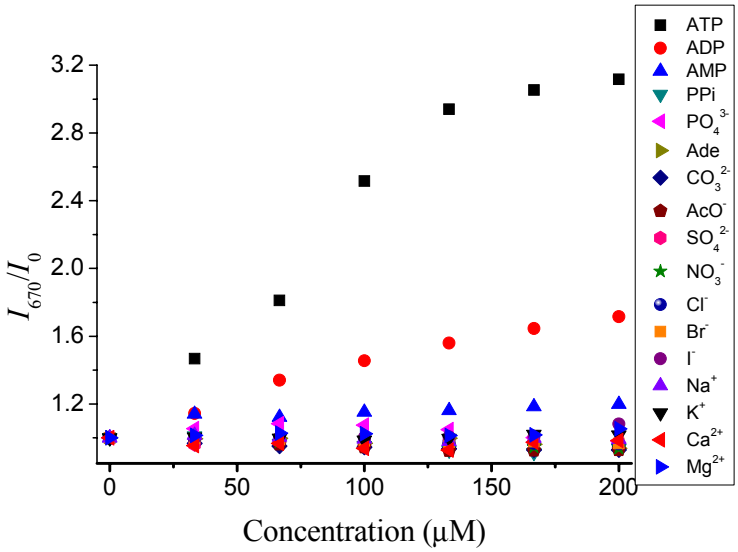

Figure S11. Relative fluorescence Ratio (I_{670}/I_0) of **SQ** (5 μM) in presence of CTAB (333 μM) in phosphate buffer (10 mM, pH 7.2) upon addition of different ions (0.2 mM).

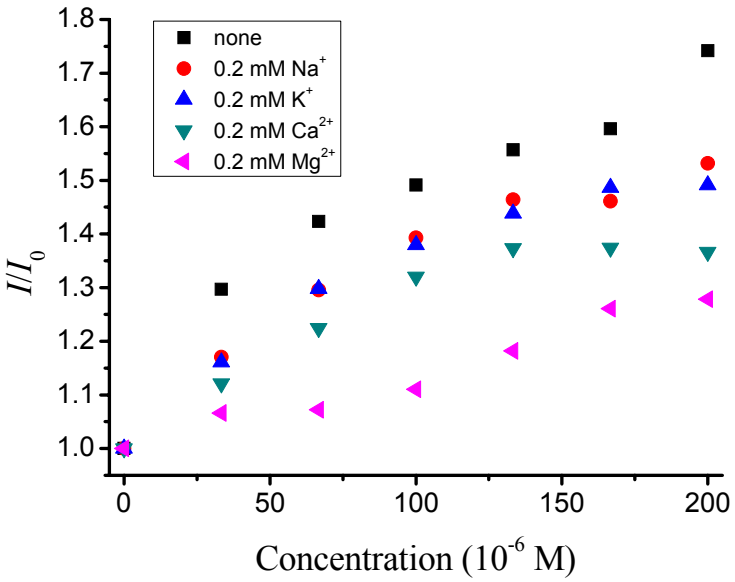

Figure S12. Relative fluorescence Ratio (I_{626}/I_0) of **SQ** (5 μM) in phosphate buffer (10 mM, pH 7.2) upon addition of ATP in the presence of various cation (0.2 mM).

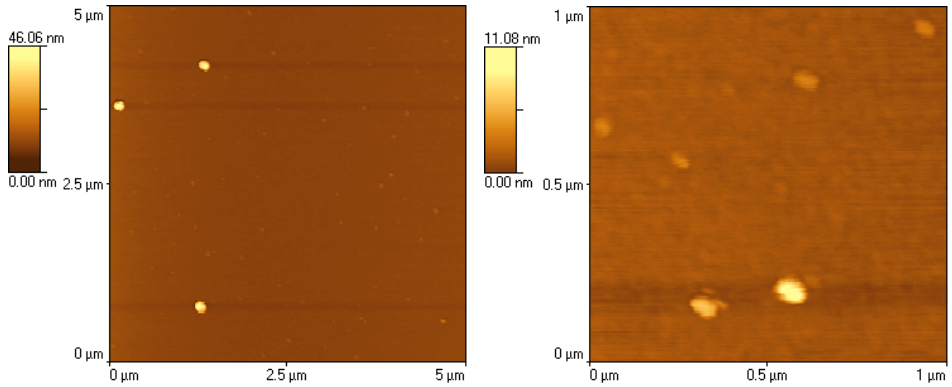

(a) images of CTAB

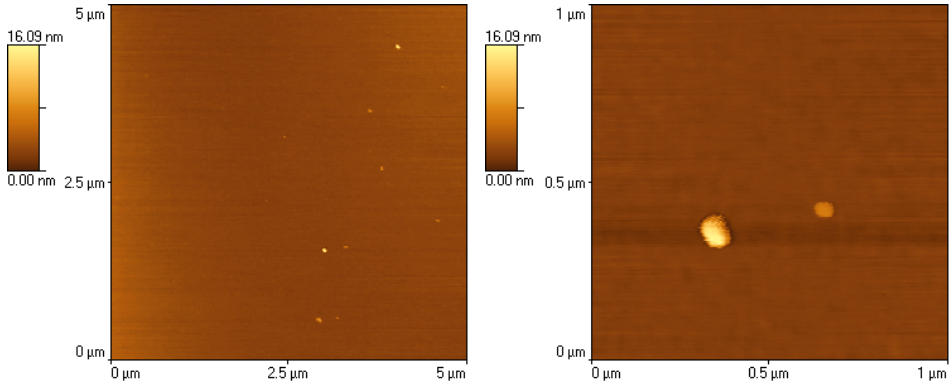

(b) images of CTAB+**SQ**

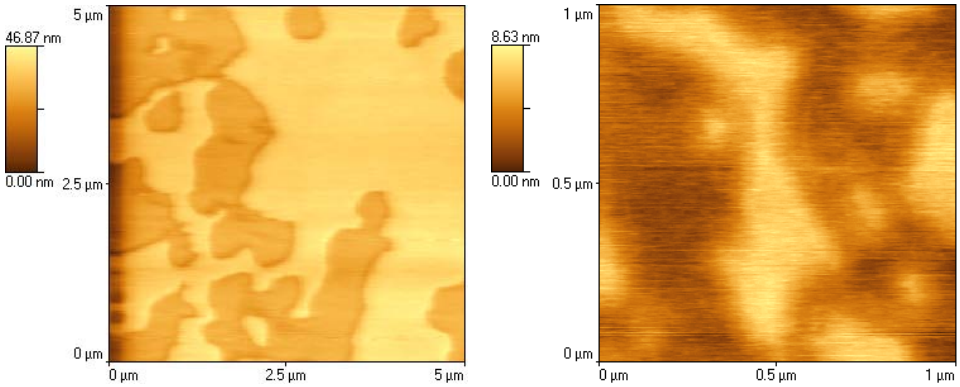

(c) images of CTAB+**SQ**+ATP

Figure S13. AFM image of CTAB, CTAB+**SQ**, CTAB+**SQ**+ATP on silica wafers.

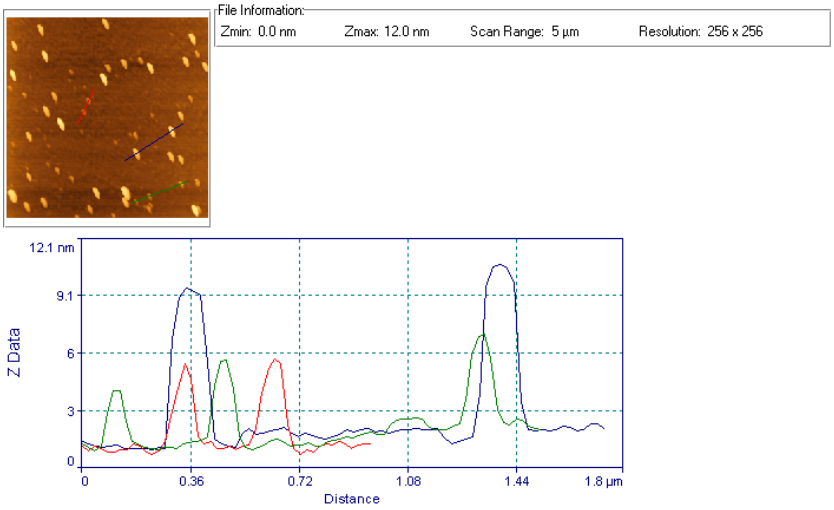

(a) images of CTAB

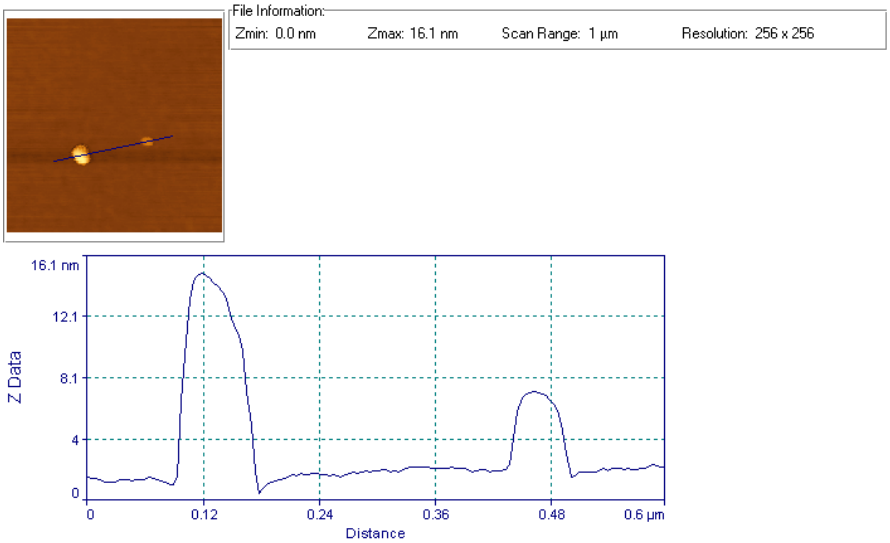

(b) images of CTAB+**SQ**

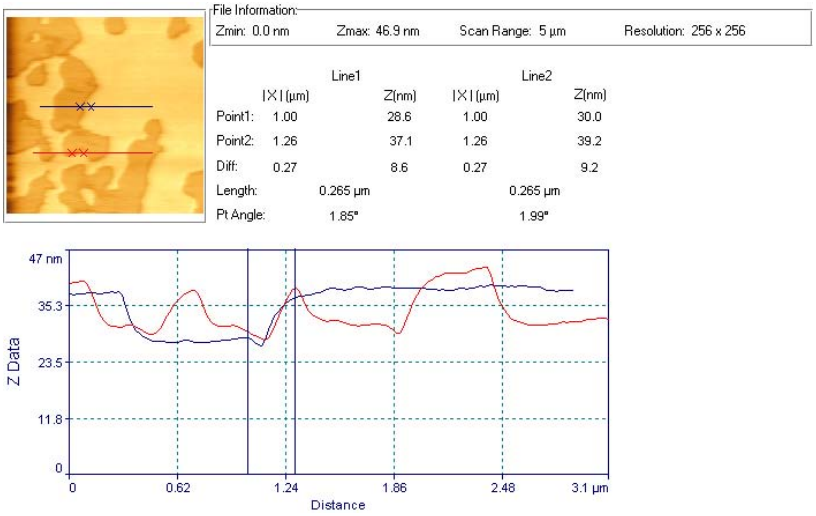

(c) images of CTAB+**SQ**+ATP

Figure S14. Tapping mode AFM image of CTAB, CTAB+**SQ**, CTAB+**SQ**+ATP on silica wafers.

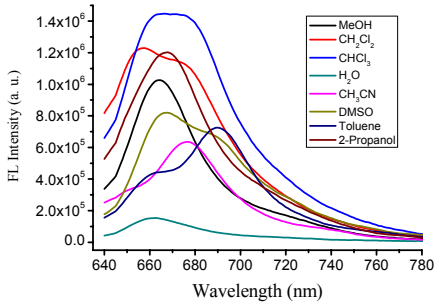

Figure S15. Emission spectra of **SQ** (5 µm) in different solvents.

Table 1. Absorption and emission data for **SQOMe** in different solvents

	λ_{max}	Em_{max}	**Φ**
CH_2Cl_2	639	656	0.032
MeOH	631	664	0.01
$CHCl_3$	642	662	0.035
CH_3CN	633	675	0.0093
Toluene	646	689	0.053
2-Propanol	635	668	0.011
DMSO	642	667	0.01
H_2O	570, 626	643	0.0066

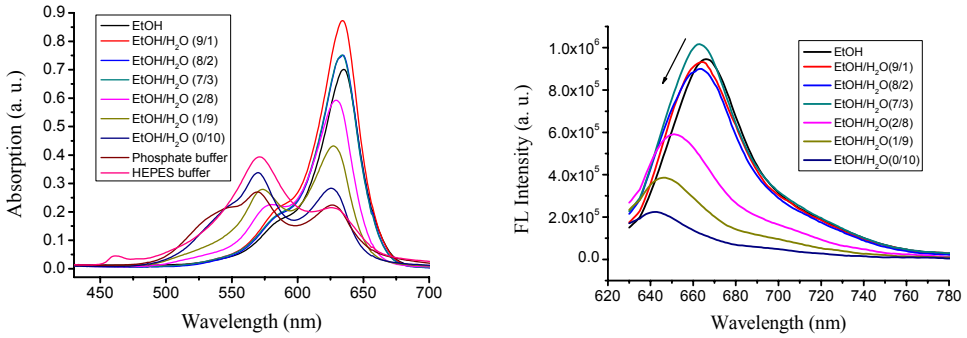

Figure S16. Absorption and emission spectra change of **SQ** (5 μm) in different aqueous solution.

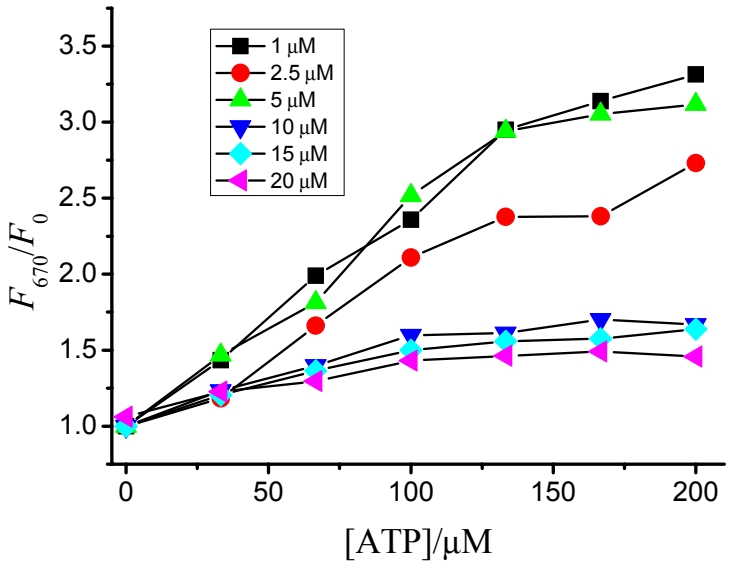

Figure S17. Relative fluorescence ratio (I_{670}/I_0) of different concentration of **SQ** in presence of CTAB (333 μM) in phosphate buffer (10 mM, pH 7.2) upon addition of ATP.

CTAB is known to form worm-like micelles upon addition of polar or charged species such as salicylate (M. Pereira, C. R. Leal, A. J. Parola and U. M. Scheven, *Langmuir*, **2010**, 26, 16715–16721). To examine whether the worm-like micelles was also contributed to the system, sodium salicylate (NaSal) was added under the same conditions. In sharp contrast to ATP, salicylate failed to induce the J-aggregates formation, since no absorption band was observed at ~665 nm (Figure S18, S19). The result indicated that NaSal was perturbing the system in a different way, possibly via the formation of worm-like micelles. And the fluorescence enhancement occurred not via SQ J-aggregate (see Figure 2b in the main text, the J-aggregate emits at 676 nm).

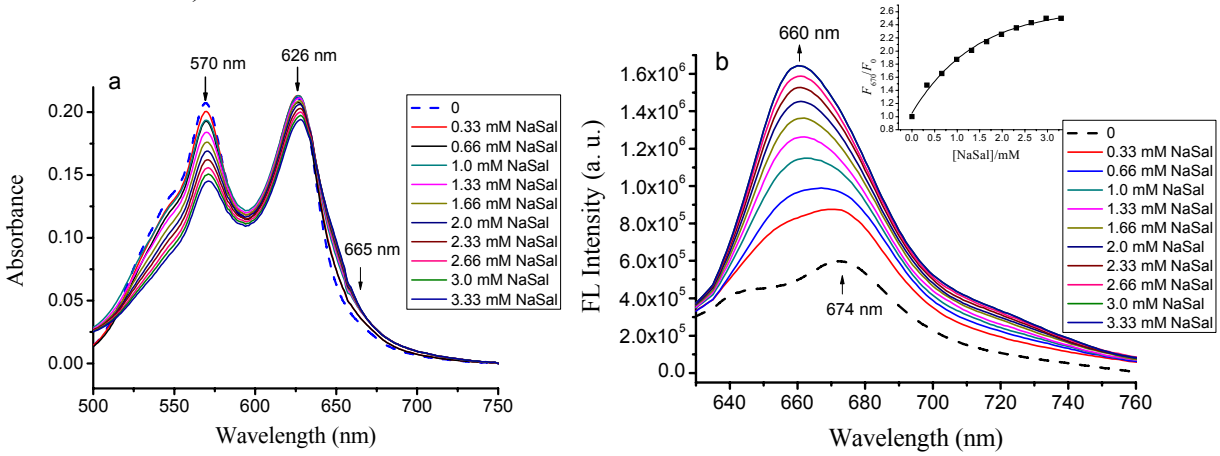

Figure S18. Absorption (a) and fluorescence (b) change of **SQ** (5 μM) in phosphate buffer (10 mM, pH 7.2) upon addition of NaSal in the presence of 333 μM of CTAB. The absorption spectrum showed no peak at ~665 nm, indicating the absence of J-aggregates.

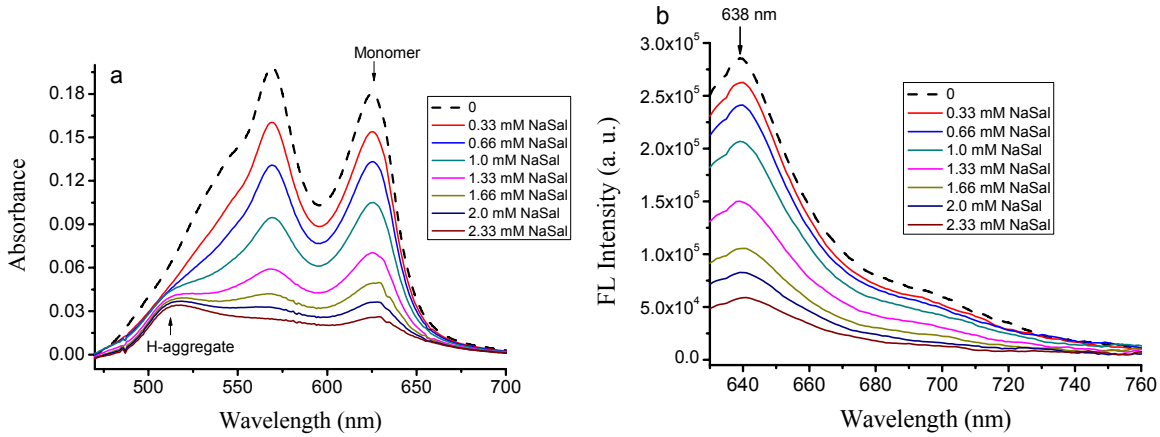

Figure S19. Absorption (a) and fluorescence (b) spectra of **SQ** (5 μM) in phosphate buffer (10 mM, pH 7.2) upon addition of NaSal in the absence of CTAB.

The π-π and electrostatic interaction between the aromatic rings of squaraine dye and NaSal induce the formation of H-aggragates and fluorescence quenching of squaraine dye.